Available online at www.sciencedirect.com
SCIENCE DIRECT
Chemical Physics Letters 421 (2006) 52–57
CHEMICAL PHYSICS LETTERS
www.elsevier.com/locate/cplett

Probing Dyson orbitals with Green's Function theory and Electron Momentum Spectroscopy

C.G. Ning [a], X.G. Ren [a], J.K. Deng [a,*], G.L. Su [a], S.F. Zhang [a], S. Knippenberg [b], M.S. Deleuze [b,*]

[a] Department of Physics and Key Laboratory of Atomic and Molecular NanoSciences of MOE, Tsinghua University, Beijing 100084, PR China
[b] Theoretical Physical Chemistry, Department of SBG, Hasselt University, Agoralaan, Gebouw D, B-3590 Diepenbeek, Belgium

Received 14 November 2005; in final form 12 January 2006
Available online 15 February 2006

Abstract

Results of an experimental study of the valence electronic structure of difluoromethane employing high-resolution Electron Momentum Spectroscopy with various impact energies are reported. One-particle Green's Function theory is utilized, for the first time, for computing accurate spherically averaged electron momentum distributions. These are derived from Dyson orbitals obtained using the third-order Algebraic Diagrammatic Construction (ADC(3)) scheme. The corresponding eigen-energies also accurately reproduce the (e, 2e) ionization spectrum. Shortcomings of empirical analyses of (e, 2e) experiments based on Kohn–Sham orbitals and eigen-energies are comparatively discussed. A failure of the target Hartree-Fock approximation is noted for the momentum distribution pertaining to the $1b_1 + 3b_2 + 5a_1$ levels.

1. Introduction

Electron Momentum Spectroscopy (EMS) is a unique technique for experimentally investigating the electronic structure of atoms and molecules in the gas phase, and of solids [1]. EMS is based on kinematically complete electron impact ionization experiments focusing on (e, 2e) reactions ($M + e^- \rightarrow M^+ + 2e^-$). In such experiments, the energies and momenta of the impinging and outgoing electrons are fully determined in coincidence. Under the assumptions of the Born, binary encounter, and plane wave impulse approximations, analysis of the angular dependence of differential cross sections at high impact energies and within a symmetric non-coplanar kinematical set up enables a mapping [1] of the ionization spectrum of the molecular target M with electron distributions derived from the Fourier Transforms in momentum (p) space of Dyson (spin-) orbitals, $g_f(\omega, r)$:

$$\sigma_f = K \int d\Omega |g_f(\omega,\ p)|^2, \tag{1}$$

with ω the spin variable (α or β). In Eq. (1), $\int d\Omega$ denotes integration over all molecular orientations in the gas phase (spherical averaging). Using spin-space coordinates $\mathbf{x} = (\omega, r)$, Dyson orbitals are defined [1,2] as partial overlaps between the neutral ground state and ionized states:

$$g_f(\mathbf{x}) = \sqrt{N} \int \Psi_f^{N-1}(\mathbf{x}_1,\ \mathbf{x}_2, \cdots, \mathbf{x}_{N-1}) \times \Psi_0^N(\mathbf{x}_1,\ \mathbf{x}_2, \cdots, \mathbf{x}_{N-1}, \mathbf{x})\, d\mathbf{x}_1\, d\mathbf{x}_2 \cdots d\mathbf{x}_{N-1}, \tag{2}$$

with N the number of electrons. Under the target Hartree–Fock (HF) [3] or Kohn–Sham (KS) [4] approximations, the measured electron momentum distributions (MDs) reduce to [5] structure factors derived as the square of HF or KS orbitals in their momentum representation. EMS is therefore very commonly regarded as a powerful *orbital-imaging* technique.

Comparisons between MDs relating to KS orbitals and to Dyson orbitals derived from benchmark Configuration Interaction [CI] calculations are too rare [6–11] to conclude

* Corresponding authors. Fax: +86 10 6278 1604 (J.K. Deng), +32 11 26 8301 (M.S. Deleuze).
E-mail addresses: djk-dmp@mail.tsinghua.edu.cn (J.K. Deng), michael.deleuze@uhasselt.be (M.S. Deleuze).

0009-2614/$ - see front matter © 2006 Elsevier B.V. All rights reserved.
doi:10.1016/j.cplett.2006.01.040

that electronic correlation is always correctly accounted for by the target KS approximation. Density Functional Theory (DFT) suffers of fundamental limitations, among which the *incorrect behavior* [12–14] *of most currently used exchange–correlation potentials in the asymptotic region* ($r \to \infty, p \to 0$), due to the unavoidable self-interaction error. The latter error is known to yield systematic underestimations, by several eVs, of ionization energies [5,15]. KS orbitals have been nonetheless very extensively used as an *empirical* tool for accurately simulating electron MDs, and this often with the help of quantitative calculations of the related ionization spectra [5,15,16] by means of one-particle Green's Function (1p-GF) theory [2,17,18], in conjunction with the third-order algebraic diagrammatic construction (ADC(3)) scheme [19,20]. The main scope of this work is to demonstrate that such 1p-GF/ADC(3) calculations enable *also* straightforwardly accurate computations of Dyson orbitals in momentum space, in support to a high-resolution EMS study of the valence electronic structure of difluoromethane (CH_2F_2). The quality of HF and KS orbitals is comparatively assessed.

2. Theory

As EMS, 1p-GF theory enables also a mapping, and this within an exact many-body framework, of vertical ionization energies and Dyson orbitals. In its energy representation, the advanced (A) component of the one-particle Green's Function (1p-GF) has indeed the following definition [21]:

$$G^A(\mathbf{x}_2,\ \mathbf{x}_1,\ \omega) = \sum_f \frac{g_f(\mathbf{x}_2) g_f^*(\mathbf{x}_1)}{\omega - (E_0^N - E_f^{N-1}) - i0^+}, \tag{3}$$

where the sum over f runs over all the electronic configurations of the molecular radical cation M^+. It is immediately apparent that the poles of this component of the 1p-GF give access to ionization energies, whereas the corresponding residues relate to products of Dyson orbitals and to ionization intensities [17] therefore.

Employing the formalism of second quantization, Dyson orbitals can be expanded as *linear combinations* of canonical (i.e. orthonormal) occupied and unoccupied HF orbitals, $\phi_i(\mathbf{x})$, with Feynman–Dyson transition amplitudes, X_{fi}, as weight coefficients:

$$g_{\mathrm{f}}(\mathbf{x}) = \sum_i \phi_i(\mathbf{x}) \langle \Psi_f^{N-1} | a_i | \Psi_0^N \rangle = \sum_i X_{\mathrm{fi}} \phi_i(\mathbf{x}). \tag{4}$$

The norms, Γ_{f}, of Dyson orbitals define spectroscopic pole strengths, which provide a straightforward estimate of relative ionization intensities, regardless of cross section effects.

$$\Gamma_{\mathrm{f}} = \sum_i |X_{\mathrm{fi}}|^2 \tag{5}$$

At the ADC(3) level, one-electron and shake-up ionization energies are obtained as eigenvalues ($\boldsymbol{E}$) of a secular matrix ($\boldsymbol{H}$) cast over the one-hole (1h) and two-hole/one-particle (2h1p) excited (shake-*up*) configurations of the radical cation M^+, as well as 1p and 2p1h (shake-*on*) anionic configurations produced by electron attachment processes on M [19]. The sets of Feynman–Dyson transition amplitudes ($\boldsymbol{X}$) required to expand Dyson orbitals derive [2,5] from the 1h and 1p components of the associated eigenvectors ($\boldsymbol{HX} = \boldsymbol{XE}$, $\boldsymbol{X}^\dagger\ \boldsymbol{X} = \boldsymbol{1}$). By virtue of its treatment of *static* and *dynamic* self-energies, through fourth- and third-order in correlation, respectively, the 1p-GF/ADC(3) approach predicts vertical one-electron ionization energies within accuracies of ~0.2 eV [15,16]. In contrast with comparable MR-SDCI (Multi-Reference Single and Double CI) treatments [11], the 1p-GF/ADC(3) scheme is size-consistent [22] and applicable therefore to extremely large systems [23]. Unlike DFT calculations employing standard functionals, a charge-consistent ADC(3) scheme guarantees that the associated scattering potentials have the correct scaling in the asymptotic region [22].

We wish to note that in a *quasi-particle depiction* (such as the Outer Valence Green's Function scheme [17]), the 1p-GF is *assumed to be* diagonal, and Dyson orbitals *become proportional to* HF orbitals, with $\sqrt{\Gamma_{\mathrm{f}}}$ as weight coefficient. At zeroth-order in correlation (*Koopmans theorem*), Dyson orbitals *are equal to* HF orbitals ($\Gamma_{\mathrm{f}} = 1$). Similarly, KS orbitals used to expand the electron density of a *N-electron interacting* system *can be mapped onto* the Dyson orbitals of a (*hypothetical*) *non-interacting* system [24]. However, no theory so far ever proved that a formal relationship exists between the Kohn–Sham and Dyson orbitals of a *correlated* system in its *neutral* ground state. Even DFT calculations employing an *exact* functional would *not* provide the Dyson orbitals of such a system! These calculations are not suited for coping with configuration interactions in the *cation* and with the dispersion of the ionization intensity into a formally infinite number of shake-up satellites. It is therefore improper to repeatedly suggest [25] that Dyson orbitals can be *generated from* DFT calculations employing exact or, worst, *approximate* functionals!

3. Computational details

To assess the influence of the basis set in computations of orbital MDs, we compare HF or DFT results obtained using Dunning's correlation consistent polarized valence basis sets of double [or triple] zeta quality (aug-cc-pVXZ, X = D[T]) and augmented by a set of s, p, [d] and s, p, d, [f] diffuse functions on hydrogens, and carbons or fluorines, respectively [26]; as well as Dunning's cc-pVTZ basis [26] augmented by a set of s, p and s, p, d diffuse functions only on hydrogens, and carbons or fluorines, respectively (cc-pVTZ++). The ADC(3) calculations have been completed by means of the original code interfaced to the GAMESS92 package of programs [27]. KS and HF orbital MDs have been generated from DFT or HF calculations employing GAUSSIAN98 [28]. The DFT calculations have been performed using the standard gradient-corrected Becke–Perdew (BP86) functional, and its extension, the hybrid

Becke–Perdew-3-parameters-Lee–Yang–Parr (B3LYP) functional [28]. All spherically averaged orbital MDs have been obtained using the HEMS program [29] and convolved according to the experimental momentum resolution [30].

4. Experiment

The employed EMS spectrometer has been described in detail elsewhere [31]. This spectrometer employs a symmetric non-coplanar geometrical set up, and a kinematics which ensures therefore clean 'knockout' collision events. A double toroidal analyzer equipped with a series of conical retarding lenses is used for electron energy and angle analyzing, and the electron position detection and data acquisition are realized by using a pair of wedge strip anode position sensitive detectors with a Universal Serial Bus multiparameter data-acquisition system [32]. According to tests on argon and helium, the energy and time resolutions are around 1.2 eV and 2 ns, respectively. Improvements of the employed multi-angle and multi-energy detection techniques greatly increased the detection rate of (e, 2e) events in coincidence, by two orders of magnitude higher compared with our previous spectrometer [33]. In order to identify possible failures of the PWIA approximation, the electron MDs of CH_2F_2 have been measured at impact energies (E_i) of 600, 1200 and 1600 eV (+ electron binding energy). At these energies, the resolution on momenta correspondingly amounts to 0.11, 0.17 and 0.20 a.u. (1 a.u. $= \hbar a_0^{-1}$ with a_0 the Bohr radius).

5. Results and discussion

The experimental electron density distribution map of CH_2F_2 at $E_i = 1600$ eV is illustrated in Fig. 1a. An average ionization spectrum is obtained from this map (Fig. 1b) by summing measurements over all ϕ angles. This spectrum is assigned by comparison with a simulation drawn from our best ADC(3)/cc-pVTZ++ theoretical results (Fig. 1c; averaged accuracy on one-electron ionization energies: ~0.2 eV, to compare with errors of ~3 to ~4 eV for B3LYP or BP86 orbital estimates). Only 1h states ($\Gamma_f > 0.8$) produced by the removal of an electron from the $2b_1$ or $4a_1$ orbitals can be individually resolved at ~13.3 and ~24.9 eV, respectively. In the outer-valence region, two further bands at ~15.4 and 19.1 eV relate to unresolved 1h states associated to the $\{4b_2, 6a_1, 1a_2\}$ and $\{1b_1, 3b_2, 5a_1\}$ sets of orbitals, respectively. A severe breakdown of the orbital picture of ionization is noticed at the ADC(3)/cc-pVTZ++ level for the innermost $2b_2$ and $3a_1$ levels, in the form (Fig. 1c) of a dispersion of the related ionization intensity over many shake-up lines with very limited intensity ($\Gamma_f < 0.17$). More specifically, at this level, 77 (71)% of the $2b_2$ ($3a_1$) ionization intensity is recovered at binding energies comprised between 36 and 43 eV in the form of 27 (33) lines with $\Gamma_f > 0.005$. Very significant band broadening is correspondingly observed on the experimental side (Fig. 1b).

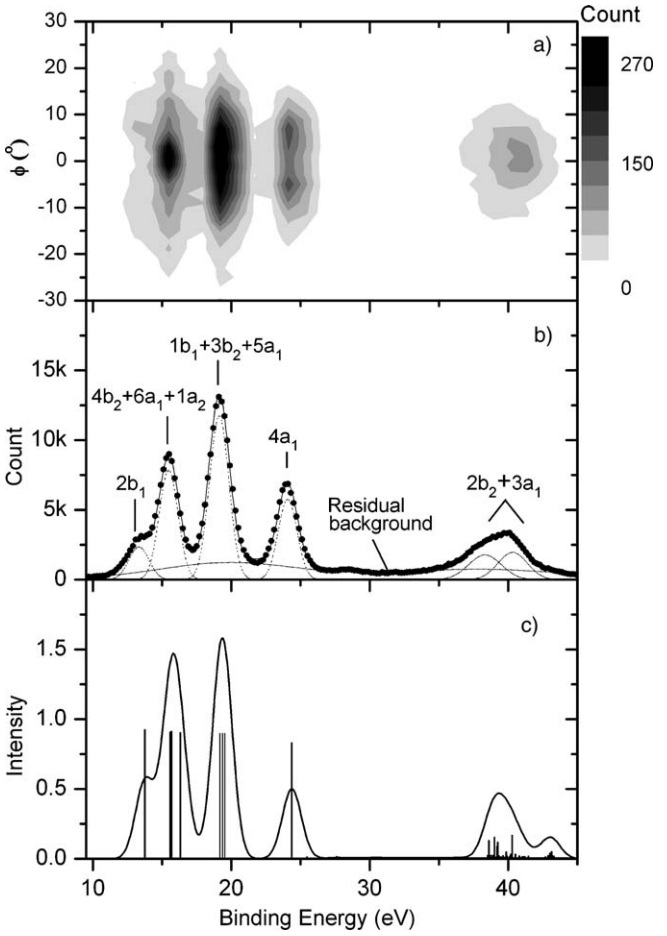

Fig. 1. (a) Angular resolved and (b) summed experimental ionization spectra of CH_2F_2 ($E_i = 1600$ eV). The dashed and full lines represent Gaussian fits and their sum, respectively. (c) ADC(3)/cc-pVTZ++ spike and convolved ionization spectra (FWHM = 1.6 eV).

Analysis of the angular dependence of the (e, 2e) intensities for the identified ionization channels provide straightforward access to the related MDs (Eq. (1)). We refer to [32] for a description of the procedure used for extracting the experimental MDs. These are compared in Figs. 2 and 3 with theoretical HF, KS, or ADC(3) Dyson orbital MDs. These theoretical MDs are overall similar and in general very faithfully reproduce the experimental measurements. Noteworthy differences are nonetheless observed at electron momenta smaller than 1 a.u. – with the ADC(3) results enabling overall the best description of experiment. Note that the BP86 and B3LYP functionals produce also excellent and essentially identical results for CH_2F_2.

The HF/aug-cc-pVTZ level fails to qualitatively describe the MD associated to the $\{1b_1, 3b_2, 5a_1\}$ set (Fig. 2c), a failure which reflects very significant *electronic correlation and relaxation effects*. Indeed, in contrast, the ADC(3) MDs very correctly reproduce the experimental results for this orbital set. Such a difference between the HF and ADC(3) results for momentum distributions demonstrates that, although the corresponding ADC(3) eigenvectors

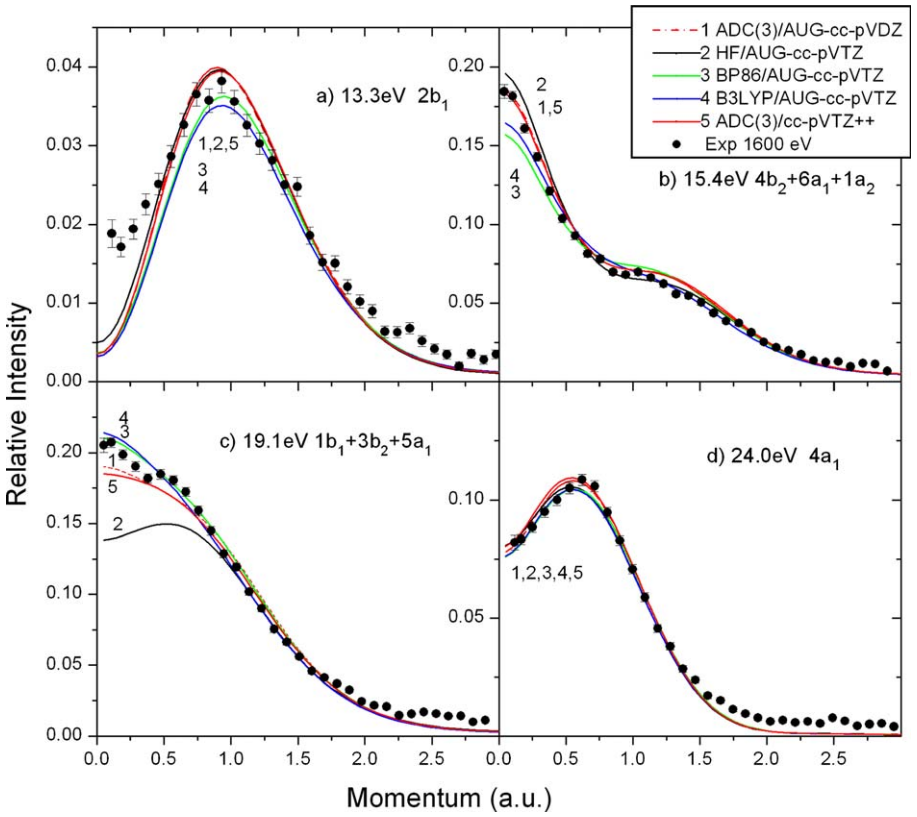

Fig. 2. Measured and calculated momentum distributions for the resolved $2b_1$, $\{4b_2 + 6a_1 + 1a_2\}$, $\{1b_1 + 3b_2 + 5a_1\}$ and $4a_1$ sets of orbitals ($E_i = 1600$ eV).

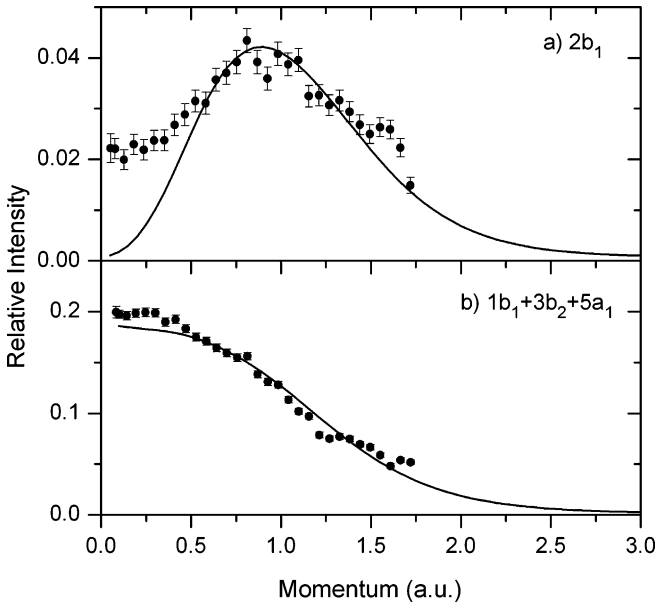

Fig. 3. Measured and ADC(3)/cc-pVTZ++ momentum distributions for the $2b_1$ and $\{1b_1 + 3b_2 + 5a_1\}$ orbital sets ($E_i = 600$ eV).

have one dominant 1h component relating to the $1b_1$, $3b_2$, or $5a_1$ HF orbitals, the contributions of many other and individually small 1h or 1p components, due to electronic relaxation in the final state or ground state correlation, respectively, may altogether significantly alter the shape of the associated Dyson orbitals, by virtue of Eq. (4). A comparison of ADC(3) results obtained using the aug-cc-pVDZ and cc-pVTZ++ basis sets confirms that the latter is large enough to ensure the convergence of the computed MDs with respect to incorporations of further atomic orbitals.

All employed models fail to reproduce the 'turn up' of the experimental MD at low electron momenta for the $2b_1$ orbital. With regards to the π*-like topology of this orbital, which exhibits two perpendicular nodal planes (Fig. 4), this discrepancy is typically due to distorted wave effects [6,34]: indeed, its extent strongly increases upon a lowering of E_i down to 1200 and 600 eV (compare Fig. 2a (1600 eV) with Fig. 3a (600 eV)). For all other orbitals the related experimental MDs are insensitive to E_i (compare e.g. Fig. 2c with Fig. 3b for the $\{1b_1, 3b_2, 5a_1\}$ set), and the plane wave impulse approximation seems therefore valid. Note that, according to He(II) measurements [35], vibrational broadening of the $2b_1$ ionization line does not exceed 0.68 eV (FWHM).

The summed ADC(3) MDs for the $\{1b_1, 3b_2, 5a_1\}$ set slightly underestimate the experimental ones at low momenta: since this set corresponds to localized (F_{2p}) lone pairs, this underestimation may be ascribed to nuclear dynamical complications. With regards to the phase relationships between their AO (atomic orbital) components, a stretching of the CF bonds, or a strong increase of the FCF bond angles are indeed expected upon ionization of

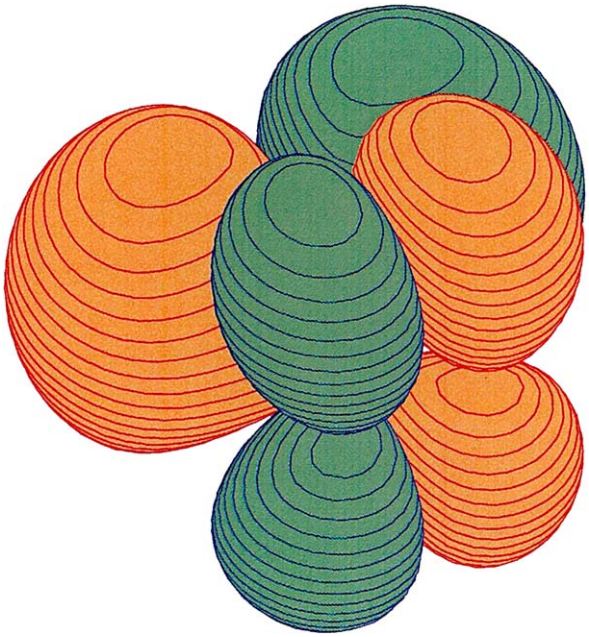

Fig. 4. Contour plot for the $2b_1$ orbital of CH_2F_2.

an electron from orbital $3b_2$, and from orbitals $1b_1$ or $5a_1$, respectively. Since in all three cases the distance between fluorine atoms increases, these distortions will result into an enhancement of the related orbital densities at large r (low p). Thus, it appears that the excellent agreement that is most usually reported between KS and experimental MDs may partly stem from a cancellation of errors (a too rapid decay of the employed exchange–correlation potentials at large distances versus the neglect of the relaxation of the electron density and of the molecular geometry).

The MD displayed at the ADC(3)/cc-pVTZ++ level for the innermost $2b_2$ and $3a_1$ valence bands (Fig. 5) has been calculated by summing the contributions from the 60 shake-up lines found at binding energies between 36 and 43 eV. For these bands, the agreement between the total ADC(3) and experimentally measured MDs is remarkable, as is the agreement of the ADC(3) MDs with the HF and KS results. This, as well as further inserts in Fig. 5 providing on an individual basis the Dyson orbital MDs associated to the 10 most intense shake-up lines, reflect the fact that Dyson orbitals for satellites related to the same electronic level have the same composition in a MO or AO basis.

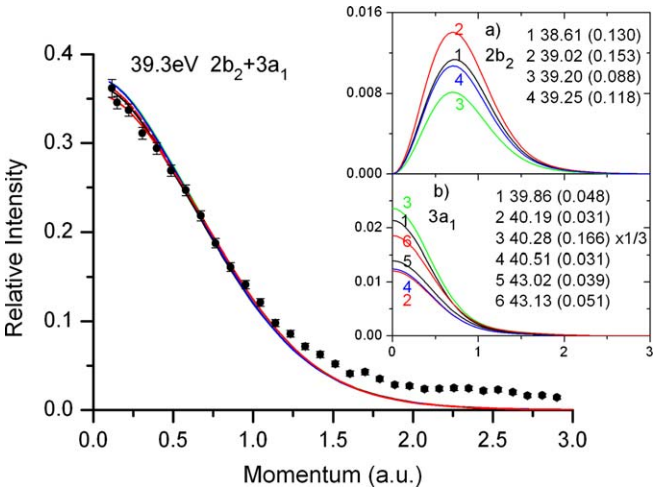

Fig. 5. Measured and calculated momentum distributions for the $2b_2 + 3a_1$ shake-up bands ($E_i = 1600$ eV), along with (insert) the ADC(3)/cc-pVTZ++ Dyson orbital momentum distributions for the 10 most intense shake-up lines (ionization energies in eV; pole strengths in parenthesis).

6. Conclusions

A link between one-particle Green's Function theory and Electron Momentum Spectroscopy has been established using Dyson orbitals derived from the ADC(3) scheme. This formalism has been applied for the first time to study the electron momentum distributions associated to the one-electron and shake-up ionization channels of difluoromethane. A comparison of ADC(3) Dyson orbital MDs with experimental or HF and KS results demonstrate the importance of static and dynamic correlation effects in (e, 2e) processes, and the advantages of a treatment of these effects by means of a *many-body* scattering potential that has the right asymptotic behavior. Besides recommending ADC(3) for quantitatively deciphering ionization spectra, this work advocates therefore a systematic use of ADC(3) Dyson orbitals in analyses of EMS experiments, in order to safely identify complications such as distorted wave effects, nuclear dynamics, or a dispersion of the ionization intensities into shake-up processes.

Acknowledgement

This project (10575062) was supported by the *National Natural Science Foundation of China* and the *Specialized Research Fund for the Doctoral Program of Higher Education* (Grant 20050003084). S.K. and M.S.D. acknowledge support by the *Fonds voor Wetenschappelijk Onderzoek_Vlaanderen* and the *Bijzonder OnderzoeksFonds* of the *Universiteit Hasselt*.

References

[1] E. Weigold, I.E. McCarthy, Electron Momentum Spectroscopy, Kluwer Academic/Plenum Publishers, New York, 1999.
[2] M.S. Deleuze, B.T. Pickup, J. Delhalle, Mol. Phys. 83 (1994) 655.
[3] Y. Zheng, C.E. Brion, M.J. Brunger, K. Zhao, A.M. Grisogono, S. Braidwood, E. Weigold, S.J. Chakravorty, E.R. Davidson, A. Sgamellotti, W. von Niessen, Chem. Phys. 212 (1996) 269.
[4] P. Duffy, D.P. Chong, M.E. Casida, D.R. Salahub, Phys. Rev. A 50 (1994) 4704.
[5] S. Knippenberg, K.L. Nixon, H. Mackenzie-Ross, M.J. Brunger, F. Wang, M.S. Deleuze, J.-P. François, D.A. Winkler, J. Phys. Chem. A 109 (2005) 9324.
[6] S.W. Braidwood, M.J. Brunger, D.A. Konovalov, E. Weigold, J. Phys. B 26 (1993) 1655.
[7] J. Rolke, N. Cann, Y. Zheng, B.P. Hollebone, C.E. Brion, Y.A. Wang, E.R. Davidson, Chem. Phys. 201 (1995) 1.

[8] P. Duffy, Can. J. Phys. 74 (1996) 763.
[9] J. Rolke, C.E. Brion, Chem. Phys. 207 (1996) 173.
[10] J. Rolke, Y. Zheng, C.E. Brion, Z. Shi, S. Wolfe, E.R. Davidson, Chem. Phys. 244 (1999) 1.
[11] Y. Zheng, W.N. Pang, R.C. Shang, X.J. Chen, C.E. Brion, T.K. Ghanty, E.R. Davidson, J. Chem. Phys. 111 (1999) 9526.
[12] M.E. Casida, C. Jamorski, K.C. Casida, D.R. Salahub, J. Chem. Phys. 108 (1998) 4439.
[13] D.J. Tozer, N.C. Handy, J. Chem. Phys. 109 (1998) 10180.
[14] J. Reimers, Z.-l. Cai, A. Bilić, N.S. Hush, Ann. NY Acad. Sci. 110 (2003) 235.
[15] S. Knippenberg, K.L. Nixon, M.J. Brunger, T. Maddern, L. Campbell, N. Trout, F. Wang, W.R. Newell, M.S. Deleuze, J.-P. François, D.A. Winkler, J. Chem. Phys. 121 (2004) 10525.
[16] W. Adcock, M.J. Brunger, I.E. McCarthy, M.T. Michaelewicz, W. von Niessen, F. Wang, D.A. Winkler, J. Am. Chem. Soc. 122 (2000) 3892.
[17] L.S. Cederbaum, W. Domcke, Adv. Chem. Phys. 36 (1977) 205.
[18] Y. Öhrn, G. Born, Adv. Quantum Chem. 13 (1981) 1.
[19] J. Schirmer, L.S. Cederbaum, O. Walter, Phys. Rev. A 28 (1983) 1237.
[20] H.G. Weikert, H.-D. Meyer, L.S. Cederbaum, F. Tarantelli, J. Chem. Phys. 104 (1996) 7122.
[21] B.T. Pickup, O. Goscinski, Mol. Phys. 26 (1973) 1013.
[22] M.S. Deleuze, Int. J. Quantum Chem. 93 (2003) 191.
[23] M.S. Deleuze, J. Phys. Chem. A 108 (2004) 9244.
[24] O.V. Gritsenko, B. Braïda, E.J. Baerends, J. Chem. Phys. 119 (2003) 1937.
[25] S. Saha, F. Wang, C.T. Falzon, M.J. Brunger, J. Chem. Phys. 123 (2005) 124315.
[26] T.J. Dunning Jr., J. Chem. Phys. 90 (1989) 1007.
[27] M.W. Schmidt et al., J. Comput. Chem. 14 (1993) 1347.
[28] M.J. Frisch et al., GAUSSIAN 98, Revision A.7, Gaussian Inc., Pittsburgh, PA, 1998.
[29] B.P. Hollebone, J.J. Neville, Y. Zheng, C.E. Brion, Y. Wang, E.R. Davidson, Chem. Phys. 196 (1995) 13.
[30] J.N. Migdall, M.A. Coplan, D.S. Hench, et al., Chem. Phys. 57 (1981) 141.
[31] X.G. Ren, C.G. Ning, J.K. Deng, S.F. Zhang, G.L. Su, F. Huang, G.Q. Li, Rev. Sci. Instrum. 76 (2005) 063103.
[32] C.G. Ning, J.K. Deng, G.L. Su, H. Zhou, X.G. Ren, Rev. Sci. Instrum. 75 (2004) 3062.
[33] J.K. Deng, G.Q. Li, Y. He, J.D. Huang, H. Deng, X.D. Wang, F. Wang, Y.A. Zhang, C.G. Ning, N.F. Gao, Y. Wang, Y. Zheng, J. Chem. Phys. 114 (2001) 882.
[34] X.G. Ren, C.G. Ning, J.K. Deng, S.F. Zhang, G.L. Su, F. Huang, G.Q. Li, Phys. Rev. Lett. 94 (2005) 163201.
[35] G. Bieri, L. Asbrink, W. von Niessen, J. Electron Spectrosc. Relat. Phenom. 23 (1981) 281.